Spin-orbit interaction and spin relaxation in a two-dimensional electron gas

M. Studer,[1,2] S. Schön,[3] K. Ensslin,[2] and G. Salis[1,*]
[1]*IBM Research, Zurich Research Laboratory, Säumerstrasse 4, 8803 Rüschlikon, Switzerland*
[2]*Solid State Physics Laboratory, ETH Zurich, 8093 Zurich, Switzerland*
[3]*FIRST Center for Micro- and Nanosciences, ETH Zurich, 8093 Zurich, Switzerland*
(Received 12 September 2008; revised manuscript received 28 November 2008; published 5 January 2009)

Using time-resolved Faraday rotation, the drift-induced spin-orbit field of a two-dimensional electron gas in an InGaAs quantum well is measured. Including measurements of the electron mobility, the Dresselhaus and Rashba coefficients are determined as a function of temperature between 10 and 80 K. By comparing the relative size of these terms with a measured in-plane anisotropy of the spin-dephasing rate, the D'yakonov-Perel' contribution to spin dephasing is estimated. The measured dephasing rate is significantly larger than this, which can only partially be explained by an inhomogeneous g factor.

DOI: 10.1103/PhysRevB.79.045302 PACS number(s): 73.21.Fg, 85.75.−d, 71.70.Ej, 78.47.−p

The possibility to manipulate spins in semiconductors is a requirement for future spin-based information processing.[1] Using the spin-orbit (SO) interaction[2,3] is a promising way to precisely control spin polarization because of its simple principle based on external gate electrodes.[4,5] Manipulation of spins using the SO interaction has been shown in various semiconductor systems, such as bulk semiconductors,[6] two-dimensional electron gases[7] (2DEGs), and even quantum dots containing only one single electron.[8] On the other hand, the SO interaction is a source for spin dephasing. In 2DEGs, the SO interaction induces a linear k-dependent splitting.[9] This splitting gives rise to an effective magnetic field, leading to dephasing of the polarized electron spins.[10] This effect is known as the D'yakonov-Perel' (DP) mechanism, and its control through manipulation of the SO interaction has been proposed[11] as an alternative to the ballistic spin transistor.[4] A careful engineering of the SO interaction is therefore crucial for using it to manipulate the spin.

In a 2DEG at intermediate temperatures, it is often assumed that the spin decay is governed by the DP mechanism.[12,13] Based on this assumption, information on the SO interaction in semiconductor quantum wells (QWs) was obtained from measurements of the spin-dephasing rate.[14–16] An independent measurement of the relative size of the SO interaction in (110)-grown QWs using the photogalvanic effect has been described in Ref. 17 and compared to the spin decay time. In this paper, we report on quantitative and independent measurements of the SO interaction and the spin-dephasing rate in an InGaAs QW, utilizing time-resolved Faraday rotation. In a further development of the method described in Ref. 7, a well-defined current is applied in the 2DEG using ohmic contacts and a mesa structure (in Ref. 7, the electron drift was induced by an ac voltage applied to Schottky contacts in an unstructured 2DEG). The drifting electrons see an effective SO magnetic field, in the following referred to as drift SO field. The sizes of its two contributions, the Rashba[3] and the Dresselhaus[2] fields, are determined as a function of temperature T from the measured influence of the in-plane electron drift velocity on the spin precession. Comparing our results with measured spin-dephasing rates and their in-plane anisotropy, we find that DP is not the only mechanism for spin decay in our samples at T between 10 and 80 K.

The 2DEG we use in this work is located in an $In_{0.1}Ga_{0.9}As/GaAs$ QW. Electrons are confined to a 20-nm-thick $In_{0.1}Ga_{0.9}As$ layer that is n-doped (3×10^{16} cm^{-3}) to ensure a small electron scattering time such that we are in the dirty limit of the SO interaction,[9] where the frequency ω_{SO} of spin precession about the SO fields is small compared with the momentum scattering rate $1/\tau_p$ ($\omega_{SO}\tau_p \approx 10^{-5}$ for our samples). On both sides of this layer, there is a 10-nm-thick GaAs spacer layer and a 10-nm-thick layer of n-doped GaAs. A 10 nm cap of undoped GaAs completes the structure, grown by molecular beam epitaxy and forming a 2DEG 40 nm below the surface. We use wet etching to pattern a cross-shaped mesa as shown in Fig. 1(a) and create standard AuGe ohmic contacts in the four ends of the cross. Four additional contacts on one arm of the cross allow its use as a Hall bar to determine the resistivity and carrier density of the 2DEG. Two samples with the same structure are glued into one chip carrier, whereby one sample is rotated by 90° to allow the SO interaction to be measured in one cool down. At 40 K, the two-point resistance of the crosses in the $\boldsymbol{x}$ or $\boldsymbol{y}$ direction is 4.1 kΩ. We use additional resistors R_s=4.7 kΩ to compensate for small variations in the contact resistance and apply voltages $V_1=V_A\cos(\phi)$ and $V_2=V_A\sin(\phi)$ as shown in Fig. 1(a). All angles are given with respect to the x axis along

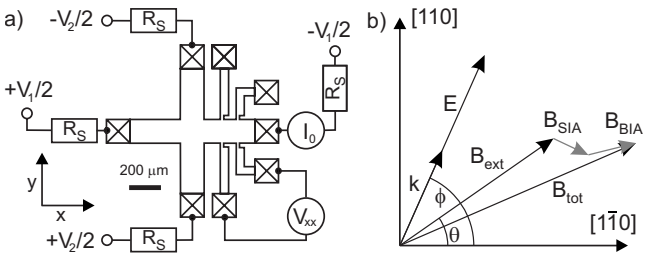

FIG. 1. (a) The InGaAs/GaAs QW is shaped into a cross with 150-μm-wide arms contacted by ohmic contacts. Additional contacts on one arm of the cross allow a four-point measurement of the voltage drop V_{xx} and the determination of electron sheet density and mobility. (b) θ and ϕ are the angles of the magnetic and electric fields with respect to the [1$\bar{1}$0] axis. $\boldsymbol{B}_{tot}$ is the vector sum of the external magnetic field and the two SO effective magnetic field contributions.

$[1\bar{1}0]$, as seen in Fig. 1(b). We obtain the resistivity of the 2DEG during optical experiments monitoring the ratio of the voltage drop V_{xx} and the current I_0 through one arm of the mesa [see Fig. 1(a)] and measure a value of 770 Ω/sq at 40 K. The voltages V_1 and V_2 create an electric field $\boldsymbol{E}$ in the center of the cross in direction ϕ and with an amplitude proportional to V_A. Because V_{xx} is monitored, the corresponding component of $\boldsymbol{E}$ can be determined directly (see below). The electric field shifts the Fermi circle by an amount of $\delta\boldsymbol{k}=m^*\mu\boldsymbol{E}/\hbar$, where m^* is the effective electron mass, μ is the electron mobility, and $\hbar$ is Planck's constant divided by 2π. In the dirty SO limit, the shift induces drift SO fields that can be expressed as[9]

$$\boldsymbol{B}_{\mathrm{SIA}}=\frac{2\alpha}{g\mu_B}\begin{pmatrix}\delta k_y\\ -\delta k_x\end{pmatrix},\quad \boldsymbol{B}_{\mathrm{BIA}}=\frac{2\beta}{g\mu_B}\begin{pmatrix}\delta k_y\\ \delta k_x\end{pmatrix}, \tag{1}$$

with $\delta\boldsymbol{k}=(\delta k_x,\delta k_y)$, g is the electron g factor, μ_B is the Bohr magneton, and α and β are the Rashba and Dresselhaus spin-orbit coefficients, respectively. The Rashba field has its origin in the structure inversion asymmetry (SIA) due to nonuniform doping on both sides of the QW and the presence of the surface on one side of the QW. The Dresselhaus field is a consequence of the bulk inversion asymmetry (BIA) of the zinc-blende structure. Cubic Dresselhaus terms do not change the linearity of $\boldsymbol{B}_{\mathrm{BIA}}$ in δk but introduce a correction of $1-\frac{1}{4}k_F^2/\langle k_z^2\rangle$, where k_F is the Fermi wave number and $\langle k_z^2\rangle$ the expectation value of the squared wave number along the growth direction z. Taking a sheet density of 5.2×10^{15} m^{-2} (see below) and approximating $\langle k_z^2\rangle$ by $(\pi/w)^2$, where $w=20$ nm is the QW width, we obtain $k_F^2\approx1.32\langle k_z^2\rangle$. This gives a correction in β of about 35%, which will be neglected in the following.

An external magnetic field B_{ext} is applied in the direction θ as seen in Fig. 1(b). If not stated otherwise, we choose $B_{\mathrm{ext}}=0.987$ T. The angles θ are 90° for sample 1 and 180° for sample 2. A transverse electron polarization precesses coherently about the vector sum[18–20] of $\boldsymbol{B}_{\mathrm{ext}}$ and the drift SO fields defined in Eq. (1) with a frequency given by the modulus of this total field vector. If $B_{\mathrm{ext}}\gg B_{\mathrm{SIA}},B_{\mathrm{BIA}}$, the total field can be approximated as[7]

$$B_{\mathrm{tot}}(\theta,\phi)\approx B_{\mathrm{ext}}+(B_{\mathrm{BIA}}+B_{\mathrm{SIA}})\cos\theta\sin\phi + (B_{\mathrm{BIA}}-B_{\mathrm{SIA}})\sin\theta\cos\phi. \tag{2}$$

Because of the different angular dependencies of the Rashba and Dresselhaus SO fields, the two contributions can be distinguished. We use time-resolved Faraday rotation to determine the Larmor frequency $\Omega_L=g\mu_BB_{\mathrm{tot}}/\hbar$ of the spins precessing about $\boldsymbol{B}_{\mathrm{tot}}$. For this, the output of a pulsed Ti:sapphire laser with a repetition rate of 80 MHz is split into a pump and a probe beam. The pump/probe intensity ratio is 10/1 and, unless stated otherwise, the pump power is 500 μW, focused onto a spot 30 μm in diameter. The circularly polarized pump pulse is tuned to the absorption edge of the QW at 1.44 eV and creates a spin polarization along the growth axis of the QW. With a pump power of 500 μW and assuming an absorption of about 1%,[21] we obtain a photoexcited carrier concentration on the order of a few 10^{10} cm^{-2}, which is more than a magnitude smaller than the equilibrium carrier sheet density in the QW (see below). The Faraday rotation of the linear polarization axis of the probe pulse transmitted is proportional to the spin polarization along the QW growth axis. Changing the delay Δt between pump and probe reveals the spin dynamics of the system, and the Faraday rotation angle can be described by $A\exp(-\Delta t/T_2^*)\cos(\Omega_L\Delta t)$. Here, A is the amplitude of the Faraday signal and T_2^* the spin-dephasing time. A measurement of Ω_L in a known magnetic field reveals an electron g factor of -0.29, assuming that the g factor is negative.

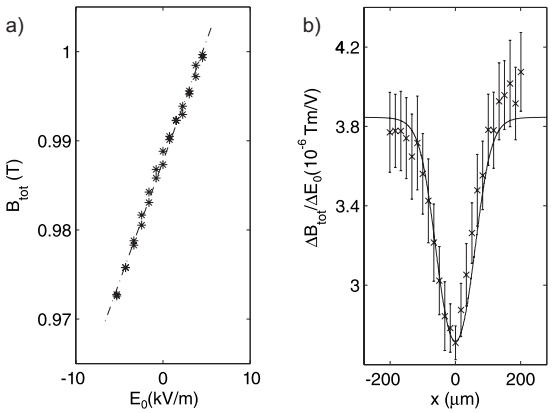

FIG. 2. (a) $|\boldsymbol{B}_{\mathrm{tot}}|$ in the center of the cross (symbols) as a function of the measured electric field. The slope of the fitted line is 2.71×10^{-6} Tm/V. (b) Dependence of the fitted slope on the position x (crosses). Assuming a constant $\alpha-\beta$ of 4.9×10^{-14} eV m, a simulation of the electric field reproduces the measured values (solid line).

Figure 2(a) shows B_{tot} measured in the center of the cross as a function of the electric field $E_0=V_{xx}/l$ between the two contacts in the right arm. These contacts are separated by a distance of $l=100$ μm. V_2 is set to ground. The temperature of the sample is 40 K, and B_{ext} is oriented along the [110] direction, therefore $\theta=\phi=90°$. The data in Fig. 2(a) contain values from sweeps of V_1 up and down. The up and down sweeps fit nicely to a straight line, showing that we can exclude a drift of Ω_L over time, which might be caused by nuclear polarization, or a drift of laser power or temperature.

As a result of the sample geometry and the grounded contacts to the left and the right of the center, the electric field in the center of the cross is reduced as compared to the value E_0 measured in the arm. By scanning the laser beam along the x axis and centered in the y direction [see Fig. 1(a)], we obtain a cross section of the drift SO field that is related to the electric-field distribution.[22] The resulting slopes of the linear fits of B_{tot} vs E_0 are shown as a function of x in Fig. 2(b). We see a pronounced dip in the center of the cross, which is explained by the reduced electric field. The solid line in Fig. 2(b) represents the solution of a numeric simulation of the electrostatics using a two-dimensional partial differential equation solver. Assuming that α and β are independent of the position and using the measured mobility (see below), the only fit parameter left is the difference $\alpha-\beta$. The measurement and the simulation are consistent and show that the electric field E in the middle of the cross is 0.71 times smaller than the measured value E_0. This correction is taken into account in the following when indicating electric-field values.

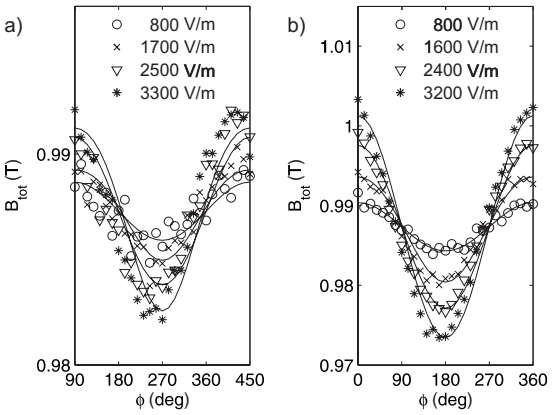

FIG. 3. B_{tot} as a function of the direction ϕ of the in-plane electric field for different amplitudes E and for two external magnetic field directions (a) $\theta=180°$ and (b) $\theta=90°$. The solid lines are fits using Eq. (2). The data are obtained at $T=20$ K.

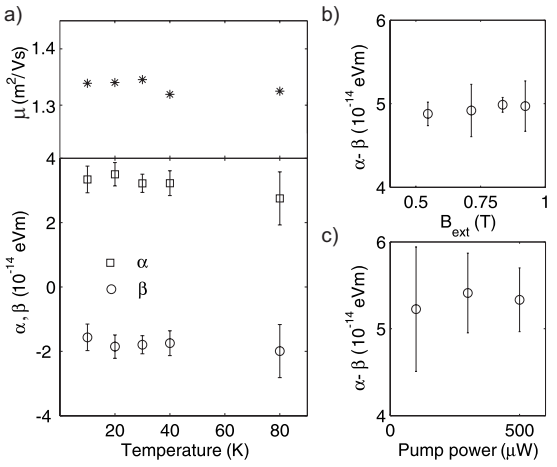

FIG. 4. (a) Measured μ, α, and β vs T. (b) Measured $\alpha-\beta$ shows no significant dependence on B_{ext}. (c) Pump-power dependence of $\alpha-\beta$. The data in (a) and (b) were obtained with a pump power of 500 μW; the data in (b) and (c) at $T=40$ K.

To disentangle α and β, we position the laser spot in the center of the cross and rotate the electric field. We did such experiments for different amplitudes of the electric field up to 3.3 kV/m and for two different configurations of $\boldsymbol{B}_{\mathrm{ext}}$. In Fig. 3(a), $\theta=180°$, and in Fig. 3(b), $\theta=90°$. The data are obtained at 20 K. B_{tot} oscillates in ϕ with an amplitude that is proportional to $\alpha+\beta$ for $\theta=180°$ and to $\alpha-\beta$ for $\theta=90°$. The difference in the amplitude for the two cases (note the different scales) shows that B_{SIA} and B_{BIA} are comparable in relative strength and that the interplay of the two SO effects gives rise to an anisotropic spin splitting in k space. The solid lines are a fit to the data using Eq. (2). Small deviations of the data from theory in the ϕ direction could result from a slight accidental off-center position of the laser spot.

To calculate the SO coefficients α and β from the measured B_{SIA} and B_{BIA}, we need a value for the drift momentum of the electrons. This is obtained from a Hall measurement of the sheet resistivity ρ and the sheet carrier density n. We calculate the mobility μ using $\mu=1/ne\rho$, e being the electron charge. In the dark, the resistivity of the 2DEG is approximately 1000 Ω/sq and decreases to 770 Ω/sq under conditions of the optical measurements. The Hall sheet densities are 5.8×10^{15} m^{-2} under illumination and 4.5×10^{15} m^{-2} in the dark. These densities are constant from 10 to 80 K. From Shubnikov–de Haas oscillations at $T<20$ K, we get a sheet density of 5.2×10^{15} m^{-2} under optical illumination. A small parallel conductivity of a doping layer could explain the difference in the two numbers. Such a parallel conductivity does not influence the optical experiments as these electrons do not contribute to the Faraday signal.

The mobilities extracted from the Hall measurement under illumination are shown in the upper inset of Fig. 4(a). The mobility does not change significantly over the temperature range measured. Using the results of the transport measurements and assuming that $m^*=0.058$, we can calculate δk and use Eq. (1) to obtain α and β for all the temperatures measured. The results are displayed in Fig. 4(a). Error bars show a 2σ confidence interval. The wafer used for this work is the same as the one used for sample 3 in Ref. 7. We measure values for α and β that are by a factor of 2–3 smaller, which we attribute to a more precise determination of the electric field in this work. In addition, different wafer processing and oxidation of the wafer surface over time might influence the SO coefficients measured in this shallow 2DEG. Variations in α and β for subsequent cool downs are within the error bar. Note that we extrapolate the mobility and the electric field in the center of the cross from a transport measurement away from the center. We cannot exclude that we underestimate the absolute values for α and β because of a reduced electron drift momentum that might result from, e.g., screening by the optically excited charge carriers. The model of Viña *et al.*[23] with the results and the parameters used by Hübner *et al.*[24] predict the T dependence of the band parameters, from which we estimate the T dependence of α and β using $\boldsymbol{k}\cdot\boldsymbol{p}$ theory.[25] The calculated T-induced change in α and β between 10 and 80 K is in the subpercentage range and thus much smaller than our measurement error. Interestingly, in Ref. 15 a linear increase in α with T for higher T was observed on a [110] QW, which the authors could not explain with $\boldsymbol{k}\cdot\boldsymbol{p}$ theory.

We find no dependence of the SO coefficients on B_{ext}, in agreement with our assumption that the precession frequency is given by the modulus of the vector sum of B_{ext} and the drift SO fields given in Eq. (1). Figure 4(b) shows a measurement of $\alpha-\beta$ vs B_{ext}. The insensitivity of the result on B_{ext} excludes a significant admixture of a k-dependent and anisotropic g factor, as was stipulated in Ref. 26. To test the reliability of our method, we also checked whether a lower pump power will influence the outcome of the measurement. This could occur from, e.g., a population of higher energy states with larger pump power. We found, however, that $\alpha-\beta$ does not depend significantly on the pump power, as seen in Fig. 4(c).

When α and β are of similar magnitude, the spin lifetime is strongly anisotropic with respect to the direction of $\boldsymbol{B}_{\mathrm{ext}}$ in the plane of the 2DEG.[11,14,16,20,27,28] This anisotropy is a consequence of the DP mechanism because the spins precess about a SO field whose direction becomes independent of k for $\alpha\approx\beta$. From the measured anisotropy in T_2^* and the rela-

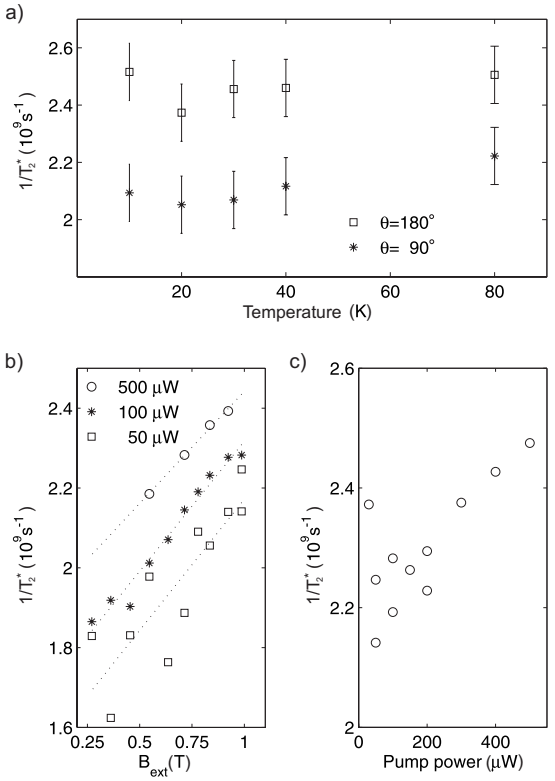

FIG. 5. (a) Spin-dephasing rate $1/T_2^*$ for two different in-plane directions θ vs T from 10 to 80 K. The average of three measurements with 50 μW pump power was used. (b) $1/T_2^*$ vs B_{ext} and linear fits for three different pump powers. The data are measured in the $\theta=90°$ configuration at 10 K and at 40 K for the 500 μW case. (c) Pump-power dependence of $1/T_2^*$ measured at 10 K in the $\theta=90°$ configuration.

tive size of α and β, we estimate the contribution from the DP mechanism to the spin dephasing. In Fig. 5(a), the spin-relaxation rate $1/T_2^*$ is plotted as a function of T for the two orientations of $B_{\text{ext}}=0.99$ T. The T dependence is rather small, and we can clearly see an anisotropy of $1/T_2^*$, confirming the anisotropic spin splitting in our system. Because our 2DEG is well in the dirty SO limit, we can use the motional narrowing limit of the DP mechanism,[9] where the spin dephasing due to $|\boldsymbol{k}|$-dependent SO fields is decreased by spin-preserving scattering. This gives the following expressions for the anisotropic spin decay rates:

$$\frac{1}{\tau_z} = C(\alpha^2+\beta^2), \quad \frac{1}{\tau_{x,y}} = \frac{C}{2}(\alpha \pm \beta)^2. \tag{3}$$

Here, $\tau_{x,y,z}$ are the relaxation times of spins oriented along x, y, or $z \| [001]$. C is a constant that depends on T, Fermi energy, scattering time, and the scattering mechanism.[29] If we apply a large external magnetic field ($\Omega_L \tau_{x,y,z} \gg 1$), we can write the DP spin-dephasing rate as[16]

$$\frac{1}{\tau_{\text{DP}}(\theta)} = \frac{1}{2}\left(\frac{1}{\tau_z} + \frac{\sin^2\theta}{\tau_x} + \frac{\cos^2\theta}{\tau_y}\right). \tag{4}$$

For the difference, we get $\frac{1}{\tau(90)} - \frac{1}{\tau(180)} = C\alpha\beta$ and read a value of about 0.4×10^9 s^{-1} in Fig. 5(a) for the difference. Using the measured values for α and β, we get $C=6.6\times10^{35}$ m^{-2} eV^{-2} s^{-1}. From Eqs. (3) and (4), this yields relaxation rates for DP of about 0.6×10^9 s^{-1} for $\theta=180°$ and of 1.0×10^9 s^{-1} for $\theta=90°$. In Eq. (3), it is assumed that the SO splitting is linear in k. As mentioned earlier, we are in a regime where $k_F^2 \approx \langle k_z^2 \rangle$. Taking into account the cubic Dresselhaus terms,[29] we find only a small correction to the values for the spin-relaxation rate obtained above. As the total $1/T_2^*$ lies between 2.1×10^9 and 2.5×10^9 s^{-1}, other spin-dephasing mechanism must be present in our sample.

To exclude optical recombination as a source of decay of the Faraday signal, we measured the time-resolved reflection,[13] which exponentially decays with a decay time of less than 100 ps (data not shown). Interpreting this time as the electron-hole recombination time provides evidence that the spin polarization, which is observable over a much longer time scale in the Faraday signal, must get imprinted onto the equilibrium electrons in the QW conductance band through recombination of unpolarized electrons and holes.[30] It is therefore justified to interpret the decay time of the Faraday signal fitted in a window from 80 to 1000 ps as the decay time T_2^*.

From the dependence of T_2^* on B_{ext}, information on the mechanism of spin dephasing can be obtained. The DP spin-dephasing rate does not depend on B_{ext} in the motional narrowing regime and for $\Omega_L \tau_p \ll 1$.[31] In contrast to this, a B dependence that is intrinsic to the DP mechanism is observed in high-mobility samples.[28] In our low-mobility samples, we find a linear increase in T_2^* with B_{ext}, as shown in Fig. 5(b). Such a linear B dependence is evidence of an inhomogeneous dephasing due to a variation Δg of the g factor in the area of the 2DEG probed, described by a dephasing rate $1/\tau_{\Delta g}$,[30,32]

$$\frac{1}{\tau_{\Delta g}} = \frac{\Delta g \mu_B B_{\text{ext}}}{2\hbar}. \tag{5}$$

We suspect that the g-factor variation could be a consequence of the in-well doping. That the sample is rather inhomogeneous is also seen in a photoluminescence experiment, in which we observe a broad luminescence peak from the QW (not shown) with a full width at half maximum of about 20 meV. We used different pump intensities and find a similar slope for the dashed linear fits in Fig. 5(b). The 500 μW measurement was done at 40 K and the other two at 10 K. From these data, we conclude that Δg is quite constant for different pump powers. From the slopes in Fig. 5(a) and using Eq. (5), we obtain $\Delta g=0.014$. Unexpectedly in a doped sample with fast electron-hole recombination, the overall spin-relaxation rate increases with increasing pump power; see Fig. 5(c). In a high-mobility sample, a decrease in the spin-relaxation rate with increasing initial spin polarization has been observed, which goes into the opposite direction.[33] In an attempt to minimize this pump-power dependence, we used a low pump power of 50 μW for the measurement in Fig. 5(a).

Table I summarizes the contributions to the anisotropic $1/T_2^*$ for $T=30$ K. The calculated sum of the relaxation rate is by about 0.8×10^9 s^{-1} lower than the measured value.

TABLE I. Contributions to the spin decay rate $1/T_2^*$ at 30 K, as estimated from the measured anisotropy of $1/T_2^*$, SO constants α and β, the B dependence of $1/T_2^*$, and the electron mobility. Measured values are obtained at a pump power of 50 μW.

Relaxation mechanism	DP	Δg	Sum	Measured
$\theta=90°\,(1/\mathrm{s})\times 10^9$	0.6	0.7	1.3 ± 0.2	2.1 ± 0.1
$\theta=180°\,(1/\mathrm{s})\times 10^9$	1.0	0.7	1.7 ± 0.2	2.5 ± 0.1

This discrepancy indicates the presence of another spin-dephasing mechanism. A possible candidate is a random SO field originating from the Coulomb potential of ionized dopants or from surface roughness of the QW. It has been pointed out that such spatial fluctuations might limit the spin lifetime for symmetric (110) QWs (Ref. 34) or in the case where $\alpha=\beta$.[35] The importance of this effect is probably smaller in our samples where both α and β are finite but not equal in size. In a small-gap semiconductor, the Elliott-Yafet (EY) mechanism contributes to the spin dephasing.[36] By estimating the importance of the EY mechanism[12] in our sample using the measured mobility and the known band parameters, we obtain a spin-relaxation rate on the order of 5×10^7 s^{-1}. This is negligibly small, but there are indications[37] that the EY spin-dephasing rate might be larger than estimated with the equation derived for a bulk semiconductor.

The weak variation in $1/T_2^*$ with T shown in Fig. 5(a) can be understood as a consequence of little temperature dependence of the individual contributions to $1/T_2^*$. As pointed out in Ref. 29, the DP dephasing rate depends only weakly on T in the degenerate regime and in the intermediate temperature range, apart from its proportionality to the electron scattering time. As our mobility is quite constant over the temperature range measured, we do not expect large variations. We observe no evidence of a dependence of the g factor spread on T. For a degenerate electron density and a constant mobility, also the T dependence of the EY mechanism should be small. The observed weak T dependence is therefore not surprising and has also been observed in other experiments.[13]

To conclude, we have measured the SO interaction coefficients α and β as a function of T and find no significant T dependence. From α and β, the measured Hall mobility and the anisotropy in $1/T_2^*$, we estimate the contribution from DP spin dephasing and find that DP alone cannot explain the measured $1/T_2^*$. From a linear increase in $1/T_2^*$ with B_{ext}, we identify an inhomogeneous broadening from a spread in the electron g factor. These effects do not account for all of the measured spin-dephasing rate. We speculate that EY or an inhomogeneous SO field might induce an additional isotropic contribution. A more detailed study of the nature of the elastic and inelastic electron-scattering mechanisms involved might facilitate an exact attribution to the different decay mechanisms.

We gratefully acknowledge helpful discussions with T. Ihn and I. Shorubalko and thank B. Küng for evaporating contact metals. This work was supported by the CTI and the SNSF.

*gsa@zurich.ibm.com

[1] D. D. Awschalom and M. E. Flatté, Nat. Phys. **3**, 153 (2007).
[2] G. Dresselhaus, Phys. Rev. **100**, 580 (1955).
[3] Y. A. Bychkov and E. I. Rashba, J. Phys. C **17**, 6039 (1984).
[4] S. Datta and B. Das, Appl. Phys. Lett. **56**, 665 (1990).
[5] K. C. Hall and M. E. Flatté, Appl. Phys. Lett. **88**, 162503 (2006).
[6] Y. Kato, R. C. Myers, A. C. Gossard, and D. D. Awschalom, Nature (London) **427**, 50 (2004).
[7] L. Meier, G. Salis, I. Shorubalko, E. Gini, S. Schön, and K. Ensslin, Nat. Phys. **3**, 650 (2007).
[8] K. C. Nowack, F. H. L. Koppens, Y. V. Nazarov, and L. M. K. Vandersypen, Science **318**, 1430 (2007).
[9] R. H. Silsbee, J. Phys.: Condens. Matter **16**, R179 (2004).
[10] M. I. D'yakonov and V. I. Perel', Sov. Phys. Solid State **13**, 3023 (1972).
[11] J. Schliemann, J. C. Egues, and D. Loss, Phys. Rev. Lett. **90**, 146801 (2003).
[12] I. Žutić, J. Fabian, and S. Das Sarma, Rev. Mod. Phys. **76**, 323 (2004).
[13] A. Malinowski, R. S. Britton, T. Grevatt, R. T. Harley, D. A. Ritchie, and M. Y. Simmons, Phys. Rev. B **62**, 13034 (2000).
[14] N. S. Averkiev, L. E. Golub, A. S. Gurevich, V. P. Evtikhiev, V. P. Kochereshko, A. V. Platonov, A. S. Shkolnik, and Y. P. Efimov, Phys. Rev. B **74**, 033305 (2006).
[15] P. S. Eldridge, W. J. H. Leyland, P. G. Lagoudakis, O. Z. Karimov, M. Henini, D. Taylor, R. T. Phillips, and R. T. Harley, Phys. Rev. B **77**, 125344 (2008).
[16] A. V. Larionov and L. E. Golub, Phys. Rev. B **78**, 033302 (2008).
[17] V. V. Bel'kov, P. Olbrich, S. A. Tarasenko, D. Schuh, W. Wegscheider, T. Korn, C. Schüller, D. Weiss, W. Prettl, and S. D. Ganichev, Phys. Rev. Lett. **100**, 176806 (2008).
[18] V. K. Kalevich and V. L. Korenev, JETP Lett. **52**, 230 (1990).
[19] H.-A. Engel, E. I. Rashba, and B. I. Halperin, Phys. Rev. Lett. **98**, 036602 (2007).
[20] M. Duckheim and D. Loss, Phys. Rev. B **75**, 201305(R) (2007).
[21] D. A. B. Miller, D. S. Chemla, D. J. Eilenberger, P. W. Smith, A. C. Gossard, and W. T. Tsang, Appl. Phys. Lett. **41**, 679 (1982).
[22] L. Meier, G. Salis, E. Gini, I. Shorubalko, and K. Ensslin, Phys. Rev. B **77**, 035305 (2008).
[23] L. Viña, S. Logothetidis, and M. Cardona, Phys. Rev. B **30**, 1979 (1984).
[24] J. Hübner, S. Dohrmann, D. Hägele, and M. Oestreich, arXiv:cond-mat/0608534 (unpublished).
[25] R. Winkler, *Spin-Orbit Coupling Effects in Two-Dimensional Electron and Hole Systems* (Springer, Berlin, 2003).
[26] A. D. Margulis and V. A. Margulis, Sov. Phys. Solid State **25**, 918 (1983).
[27] N. S. Averkiev and L. E. Golub, Phys. Rev. B **60**, 15582 (1999).

[28] D. Stich, J. H. Jiang, T. Korn, R. Schulz, D. Schuh, W. Wegscheider, M. W. Wu, and C. Schüller, Phys. Rev. B **76**, 073309 (2007).
[29] J. Kainz, U. Rössler, and R. Winkler, Phys. Rev. B **70**, 195322 (2004).
[30] J. M. Kikkawa and D. D. Awschalom, Phys. Rev. Lett. **80**, 4313 (1998).
[31] E. L. Ivchenko, Sov. Phys. Solid State **15**, 1048 (1973).
[32] Z. Chen, S. G. Carter, R. Bratschitsch, P. Dawson, and S. T. Cundiff, Nat. Phys. **3**, 265 (2007).
[33] D. Stich, J. Zhou, T. Korn, R. Schulz, D. Schuh, W. Wegscheider, M. W. Wu, and C. Schüller, Phys. Rev. B **76**, 205301 (2007).
[34] O. Z. Karimov, G. H. John, R. T. Harley, W. H. Lau, M. E. Flatté, M. Henini, and R. Airey, Phys. Rev. Lett. **91**, 246601 (2003).
[35] E. Y. Sherman and J. Sinova, Phys. Rev. B **72**, 075318 (2005).
[36] R. J. Elliott, Phys. Rev. **96**, 266 (1954).
[37] A. Tackeuchi, T. Kuroda, S. Muto, Y. Nishikawa, and O. Wada, Jpn. J. Appl. Phys. Part 1 **38**, 4680 (1999).